journal homepage: www.intl.elsevierhealth.com/journals/cmpb

Analysis of sub-anatomic diffusion tensor imaging indices in white matter regions of Alzheimer with MMSE score

*Ravindra B. Patil**, *S. Ramakrishnan*

Non Invasive Imaging and Diagnostics Laboratory, Biomedical Engineering Group, Department of Applied Mechanics, Indian Institute of Technology Madras, Chennai 600036, India

ARTICLE INFO

Article history:
Received 10 February 2014
Received in revised form 6 June 2014
Accepted 9 June 2014

Keywords:
Diffusion tensor imaging (DTI)
Alzheimer
MMSE

ABSTRACT

In this study, an attempt has been made to find the correlation between diffusion tensor imaging (DTI) indices of white matter (WM) regions and mini mental state examination (MMSE) score of Alzheimer patients. Diffusion weighted images are obtained from the ADNI database. These are preprocessed for eddy current correction and removal of non-brain tissue. Fractional anisotropy (FA), mean diffusivity (MD), radial diffusivity (RD) and axial diffusivity (DA) indices are computed over significant regions (Fornix left, Splenium of corpus callosum left, Splenium of corpus callosum right, bilateral genu of the corpus callosum) affected by Alzheimer disease (AD) pathology. The correlation is computed between diffusion indices of the significant regions and MMSE score using linear fit technique so as to find the relation between clinical parameters and the image features. Binary classification has been employed using support vector machine, decision stumps and simple logistic classifiers on the extracted DTI indices along with MMSE score to classify Alzheimer patients from healthy controls. It is observed that distinct values of DTI indices exist for the range of MMSE score. However, there is no strong correlation (Pearson's correlation coefficient '*r*' varies from 0.0383 to −0.1924) between the MMSE score and the diffusion indices over the significant regions. Further, the performance evaluation of classifiers shows 94% accuracy using SVM in differentiating AD and control. In isolation clinical and image features can be used for prescreening and diagnosis of AD but no sub anatomic region correlation exist between these features set. The discussion on the correlation of diffusion indices of WM with MMSE score is presented in this study.

1. Introduction

Alzheimer disease (AD) is a neurodegenerative disorder caused due to the loss of neurons. It is estimated that by the year 2050, one in 85 people in the world will be living with this disease [1]. It has been reported that white matter (WM) regions in brain are most affected in AD. The change in the WM atrophy is predominant in the AD patient as the disease progresses. The diagnosis of the disease at the early stage is essential as the drugs available are only effective during initial stage of the disease [2].

* *Corresponding author*. Tel.: +91 9945044299.
E-mail addresses: ravipatil3354@gmail.com (R.B. Patil), sramki@iitm.ac.in (S. Ramakrishnan) .
http://dx.doi.org/10.1016/j.cmpb.2014.06.004
0169-2607/

Diffusion tensor imaging (DTI) technique has been used to probe the integrity of WM tracts in vivo. This technique based on the probabilistic determination of diffusion of water molecule in the tissue, helps to quantify the degradation of the WM tracts. Fractional anisotropy (FA), mean diffusivity (MD), axial diffusivity (DA) and radial diffusivity (RD) are the prominent diffusion indices, which are used to ascertain the degree of the AD pathology [3,4]. AD is found to affect specific regions in WM, hence atlas-based approach has been widely used to study the white matter integrity over different regions of interest (ROI) [6].

Mini mental state examination (MMSE) [5] is used as the clinical screening test to assess the subject's basic cognitive ability in several neurodegenerative longitudinal studies. Also this measure is considered for prescreening of AD patients from healthy controls. This score varies from 0 to 30 where 30 represent Normal Control (NC). Various studies have been reported for diagnosis of AD using clinical parameters as well as image features [7,8]. Numerous machine learning techniques have been used to classify AD from controls using volumetric change in brain images, cortical thickness analysis, temporal lobe shrinkage and voxel based analysis using DTI features [9,10]. However, little importance has been given to ascertain the relation between clinical parameters and the image features to improve the diagnostic relevance.

The aim of the present study is twofold. First, to determine the correlation between DTI indices (image features) over prominent sub anatomic regions of WM and MMSE (clinical parameter) score of the subjects. Second, to ascertain the prominence of MMSE parameter along with image features for classification of AD from NC.

2. Methodology

Data used in this study is obtained from the Alzheimer's Disease Neuroimaging Initiative (ADNI) database (http://www.loni.ucla.edu/ADNI). The dataset of the second phase of ADNI2 and ADNIGO containing DTI images (87 subjects, 50 NC and 37 AD) are used with prior permission of the concerned authority.

The data obtained are preprocessed, wherein each subject's entire DWI volumes are aligned with b0 image and eddy current distortion is corrected with the help of FSL eddy-correct tool (www.fmrib.ox.ac.uk/fsl). The resulting volumes are skull stripped using robust Brain Suite tool (http://brainsuite.loni.ucla.edu/). Susceptibility artifacts induced due to echo planar imaging, are removed by aligning linearly to their respective T1-weighted structural images using FSL flirt. The images obtained were further elastically registered to T1 scans using an inverse consistent registration algorithm [13]. The process employed is depicted in Fig. 1.

The structural and physiological constraints of WM tracts imply that diffusion of water will vary in the 3-dimensional spherical space predicted by Fick's law and demonstrated by Einstein's equation [12]. Maximum flow is observed along the central axis and reduces drastically along other perpendicular co-ordinate axes. The entire diffusion image is mapped into tensor fields with each pixel being represented by an ellipsoidal voxel. Axial length of each ellipsoid represents the magnitude of diffusion at the specified voxel location. The diffusion is quantified using characteristic features calculated for the entire tensor map. The diffusion along each axis of the fiber is calculated as the length of tensor along that direction. The direction of maximum diffusion (λ_1) [6] along the fiber is estimated as DA. This gives an estimate of the primary direction of fiber structure. RD estimates the average diffusion along the other two perpendicular axes (λ_2, λ_3) [11]. MD quantifies the average diffusion along the three axes and thus gives a measure of the total diffusion for each voxel in the tensor map.

Diffusion along fibrous tracts of WM is characterized by their anisotropic properties. The Eigen values (λ_1, λ_2 and λ_3) obtained after decomposition of diffusion tensor matrix, gives a measure of the degree of anisotropy in a highly directional structure (WM tracts). FA and MD are the most commonly used features to characterize the integrity and quantify the diffusion in WM tracts. Physical state of neuronal fibers can be estimated by RD and MD. A higher value of RD indicates a thinner myelin sheath. FA is a ratio of the diffusivities along all the directions of WM tracts. The value of FA ranges from zero to one and decreases with degeneration of WM tracts. At the onset of dementia, breakdown occurs at synaptic level, which is better identified by DA, which also gives a measure of continuity of fibers. A decrease in FA may be either due to increase in RD and MD with DA being constant or it may also be due to an decrease in DA and increase in RD with MD being constant [14,15].

From the preprocessed images the diffusion tensor matrix is modeled at each voxel and further the matrix is decomposed into Eigen values (λ_1, λ_2 and λ_3) to compute following diffusion indices

$$\mathrm{FA} = \frac{3}{2} * \frac{\sqrt{(\lambda_1 - \lambda_m)^2 + (\lambda_2 - \lambda_m)^2 + (\lambda_3 - \lambda_m)^2}}{\sqrt{\lambda_1^2 + \lambda_2^2 + \lambda_3^2}} \quad (1)$$

where λ_m is given by

$$\mathrm{MD} = \lambda_m = \frac{\lambda_1 + \lambda_2 + \lambda_3}{3} \quad (2)$$

$$\mathrm{DA} = \lambda_1 \quad (3)$$

$$\mathrm{RD} = \frac{\lambda_1 + \lambda_2}{2} \quad (4)$$

The DTI maps are obtained for FA, MD, DA and RD over 50 ROI's after registering the images with JHU DTI atlas [23]. Subsequently, JHU "Eve" WM atlas labels are applied using nearest neighbor interpolation technique to extract the ROI feature values.

Furthermore, support vector machine (SVM), simple logistic and decision stumps classification algorithms are custom implemented in MATLAB. SVM works on the principle of margin maximization and is a nonlinear parametric based approach. It uses fewer samples for training and is robust to increase in feature dimension [16]. The experimental parameters set for SVM are, polynomial kernel of order 5 is used and the soft margin is set to 1. Simple logistic classifier is based on computation of probability scores to measure the relationship between categorical dependent and independent

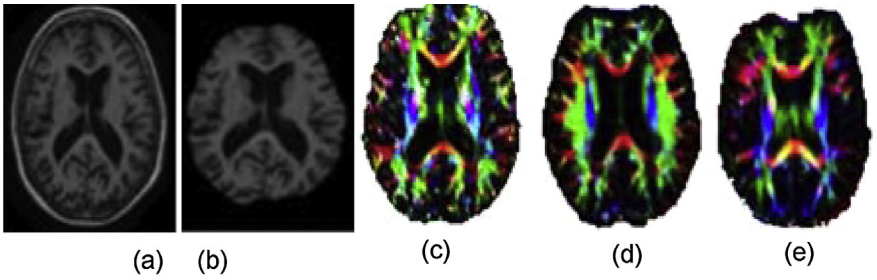

(a).Acquired Image (b).Skull Stripped Image (c) colour coded based on tracts orientation
(d) Registered Image (e) Atlas mapped Image

Fig. 1 – Workflow employed before feature extraction.

variables [17]. Ridge estimator is used in the Simple Logistic classifier with the value set to 10^{-7}. Decision stumps is a single level tree classifier, which makes prediction on the input dataset by using the predictor model [18]. The above-mentioned classifiers are selected based on the complexity of the algorithm ranging from SVM being complex to decision stumps being simple set of conditional statements. The objective is to analyze the importance of the features in predicting the outcome for both weak and robust classifiers.

Binary classification technique is employed over the features obtained from the ROI's of DTI map and MMSE score. 10 fold cross validation is used to arrive at classifiers performance for the different combinations of feature set. The performance is evaluated based on the sensitivity, specificity and accuracy of the classifiers:

$$\text{Sensitivity} = \frac{\text{TP}}{\text{TP} + \text{FN}} \tag{5}$$

$$\text{Specificity} = \frac{\text{TN}}{\text{TN} + \text{FP}} \tag{6}$$

$$\text{Accuracy} = \frac{\text{TP} + \text{TN}}{\text{TP} + \text{TN} + \text{FP} + \text{FN}} \tag{7}$$

where true positives (TP) is the number of diseased subjects correctly classified, true negative (TN) is the number of control subjects classified correctly, false positive (FP) is the number of control subjects classified as disease patients and false negative (FN) is the number of disease subjects classified as normal control.

Pearson correlation coefficient (r) is computed between the diffusion indices obtained over the significant regions and MMSE score of each subject using linear fit technique

$$r = \frac{\sum_{i=1}^{n}(X_i - \bar{X})(Y_i - \bar{Y})}{\sqrt{\sum_{i=1}^{n}(X_i - \bar{X})^2}\sqrt{\sum_{i=1}^{n}(Y_i - \bar{Y})^2}} \tag{8}$$

where $\bar{X} = (\sum_{i=1}^{n} X_i)/n$, $\bar{Y} = (\sum_{i=1}^{n} Y_i)/n$, X and Y are the sample values.

The significant regions considered in this work are Fornix, Splenium of corpus callosum and genu of corpus callosum as these are affected most due to AD pathology, which has been reported by the authors in earlier study [19].

Table 1 – The demographic and MMSE characteristics of studied group.

Groups	Number	Age	MMSE
NC	50	72 ± 17	28.98 ± 1.02
M	23	73 ± 16	29.06 ± 0.94
F	27	72 ± 14	28.9 ± 1.1
AD	37	75 ± 15	22.26 ± 5.74
M	14	76 ± 14	21.98 ± 6.12
F	13	74 ± 16	22.78 ± 5.22

3. Results and discussion

Data from 50 NC and 32 AD individuals are used for this study. Correlation between the MMSE score and DTI indices is studied for specific regions which suffered maximum damage during AD. Five of the prominent regions used for the study are: Fornix left, genu of corpus callosum left, Splenium of corpus callosum left, Splenium of corpus callosum right and bilateral genu of the corpus callosum.

The demographic diversity of subjects with age and MMSE score is presented in Table 1. The controls and AD subjects are in the same age group but the variance in MMSE score is observed to be higher for AD.

DTI indices are computed from 50 regions of WM for controls and AD data. A representative set of regions and their corresponding feature indices along with computed P value are shown in Table 3.

The comparative variation of DTI indices with MMSE scores for AD and controls for Fornix region of WM and Splenium of corpus callosum is shown in Figs. 2 and 3, respectively. Visual observation of figures indicates a clear distinction between the datasets of AD and controls. It can be inferred from the figures that distinct values of DTI indices exist for the range of MMSE score. Thus, diffusion indices and MMSE scores can be used for classification of AD. It is observed that, in AD subjects the value of FA is decreased and values of MD, RD and DA are increased compared to controls.

From Figs. 2 and 3 it could be observed that more than one unique value of DTI indices exist for the same MMSE score. This leads to poor correlation between the two. Linear fit is performed for each set of features from prominent regions and Pearson correlation coefficient 'r' value is computed, which is tabulated in Table 2. A wide range of variation in r value (0.1819 to −0.1924) exists over prominent regions for different

Table 2 – Distribution of Pearson's *r* values across prominent regions for various DTI indices.

Regions	FA		MD		RD		DA	
	AD	NC	AD	NC	AD	NC	AD	NC
Fornix left	0.038	0.13	−0.033	−0.056	0.008	−0.170	0.040	−0.035
GCC/L	0.004	0.033	−0.027	0.083	−0.048	−0.137	0.010	−0.131
SCC/L	0.181	0.059	−0.156	−0.096	−0.095	−0.111	−0.076	−0.078
SCC/R	0.146	0.025	−0.167	−0.109	−0.104	−0.055	−0.065	−0.146
BGCC	0.046	0.059	−0.025	−0.127	−0.066	−0.199	0.017	−0.192

GCC/L, genu of corpus callosum left; SCC/L, Splenium of corpus callosum left; SCC/R, Splenium of corpus callosum right; BGCC, bilateral genu of the corpus callosum.

DTI indices however no strong correlation was observed for any indices in any region with respect to MMSE.

The classification results obtained using different classifiers with varied combination of diffusion indices and MMSE score are shown in Table 4. It is observed from Table 4 that irrespective of the classifiers, the accuracy considering image features and MMSE score is over 90%. This is of no surprise as the scatter plot of different image feature values with MMSE score (Figs. 2 and 3) shows the clear boundary of separation between AD and NC data set. Considering MMSE score as an additional feature the performance of classifiers is increased by 10%. It is also interesting to note that with MMSE score, weak classifier such as Decision Stump shows a comparable performance or even better in few cases. For MD feature set, no appreciable difference in the performance of SVM classifier is observed. RD and DA feature sets follow the trend observed for FA.

Maximum classification accuracy of 94.25% (sensitivity 94.40% and specificity 93.00%) is observed for SVM classifier with FA and MMSE score as the feature set. Relative reduction in the classification accuracy is observed when only image feature sets are considered. This ascertains that MMSE score aids in improving the predictive model of the classifiers being considered.

SVM classifier is built on the strong theoretical foundation of maximizing the hyper margin by linear discrimination function. A significant change in the predictive score is needed to move the data points across the decision boundary. Hence, SVM performs better than the decision stumps and simple logistic classifiers in distinguishing AD from controls.

Further, the proposed method is compared with existing automated analysis techniques to distinguish AD from controls. It can be observed from Table 5 [24], that the efficiency of the methods using structural MRI properties is comparatively lesser than the proposed approach. Although, the multivariate approach with combination of structural and diffusion features does provide marginal improvement over the proposed approach. However, the results have to be interpreted with caution as the number of sample subjects considered in the multivariate study is comparatively lesser and also it requires high computation time and analysis to compute both structural and diffusion features. Also, the numbers of ROI's that are considered in multivariate approach are 15 and in proposed approach is only 5. Multivariate approach is dependent entirely on the imaging features whereas proposed approach incorporates the usefulness of clinical parameter.

It must be noted that although no correlation is found between image feature values and clinical screening scores,

Table 3 – Absolute values of all typical indices derived from potential regions of white matter.

Representative regions	AD				Normal controls				*P value
	FA	MD	RD	DA	FA	MD	RD	DA	
Cerebral peduncle left	0.4531	0.00104	0.00076	0.00155	0.4732	0.00100	0.00073	0.00153	0.0252
Anterior corona radiata right	0.2728	0.00099	0.00083	0.00126	0.3049	0.00089	0.00074	0.00118	0.0004
Superior corona radiata left	0.3347	0.00089	0.00072	0.00121	0.3322	0.00079	0.00065	0.00108	0.2022
Cingulum (hippocampus) left	0.2149	0.00107	0.00093	0.00127	0.2398	0.00089	0.00078	0.00111	0.0002
Cingulum (hippocampus) right	0.2441	0.00104	0.00089	0.00127	0.2645	0.00092	0.00080	0.00117	0.0233
Fornix (cres)/Stria terminalis left	0.2429	0.00154	0.00134	0.00182	0.2976	0.00115	0.00099	0.00149	0.0001
Fornix (cres)/Stria terminalis right	0.2403	0.00150	0.00131	0.00181	0.2826	0.00116	0.00100	0.00149	0.0009
Superior fronto-occipital fasciculus right	0.2123	0.00121	0.00109	0.00145	0.2518	0.00097	0.00084	0.00121	0.0003
Splenium of corpus callosum left	0.4572	0.00125	0.00092	0.00187	0.5211	0.00103	0.00071	0.00168	0.0001
Splenium of corpus callosum right	0.4677	0.00114	0.00082	0.00174	0.5242	0.00099	0.00067	0.00161	0.0001
Fornix left	0.1324	0.00274	0.00251	0.00309	0.1984	0.00225	0.00202	0.00275	0.0001
Genu of corpus callosum left	0.3935	0.00121	0.00091	0.00172	0.4515	0.00104	0.00077	0.00160	0.0001
Body of corpus callosum left	0.3569	0.00140	0.00110	0.00192	0.4018	0.00120	0.00093	0.00175	0.0082
Retrolenticular part of internal capsule left	0.4050	0.00088	0.00067	0.00127	0.4072	0.00081	0.00062	0.00119	0.9536
Tapatum right	0.2926	0.00163	0.00139	0.0021	0.3434	0.00131	0.00107	0.00178	0.0013
Bilateral body of the corpus callosum	0.3432	0.00145	0.00116	0.00195	0.3893	0.00126	0.00098	0.00180	0.0039

MD, RD and AD are measured in $mm^2\ s^{-1}$.

* *P* value is computed for FA feature set.

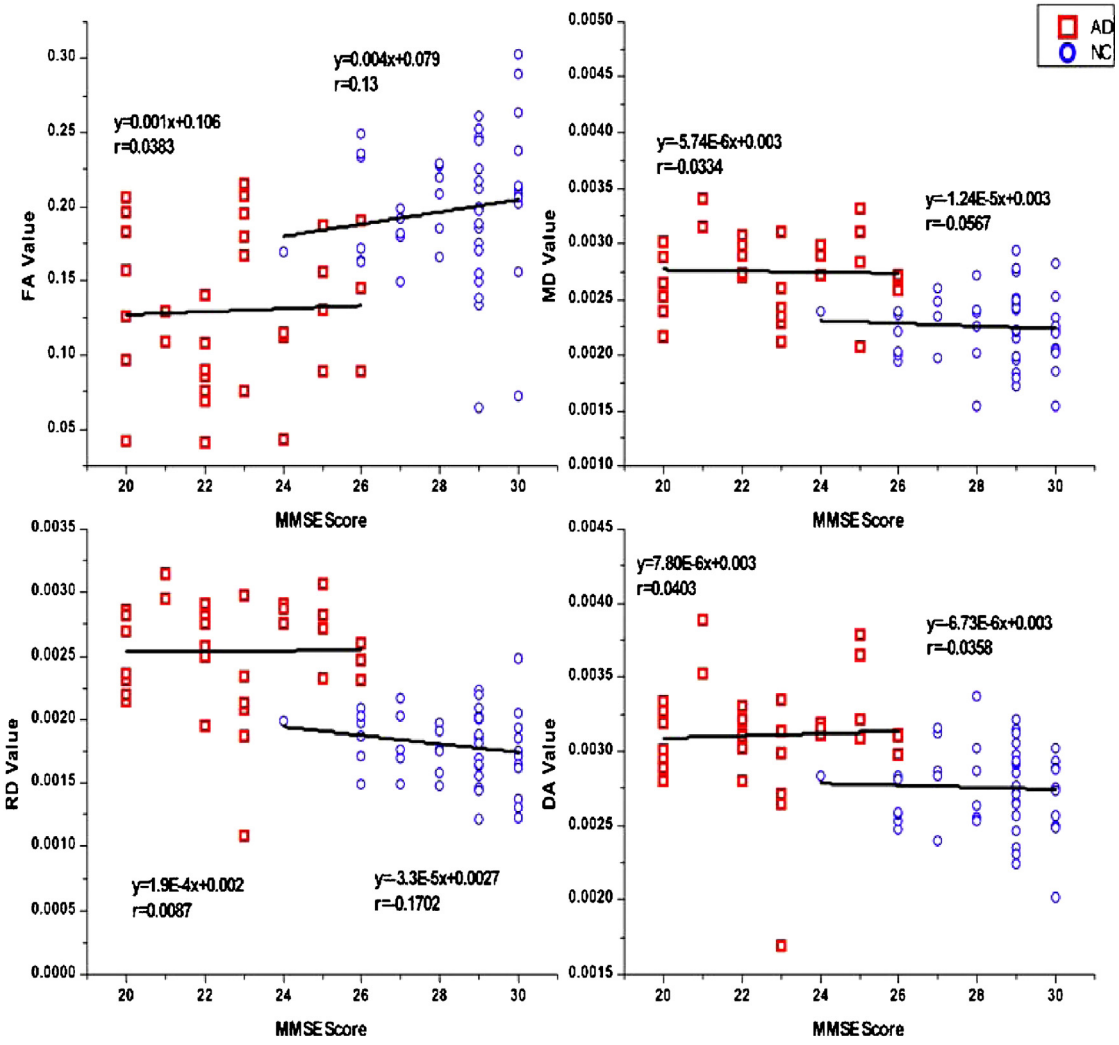

Fig. 2 – Variation of DTI indices with MMSE scores for Fornix region.

Table 4 – Performance evaluations of classifiers with and without MMSE score.

Image features	Classifier	Accuracy		Sensitivity		Specificity	
		With MMSE	Without MMSE	With MMSE	Without MMSE	With MMSE	Without MMSE
FA	SVM	94.25	81.60	94.40	81.80	93.00	81.40
	DS	93.10	70.11	91.80	72.00	94.00	69.30
	SL	94.25	78.16	97.00	75.00	90.70	80.30
MD	SVM	89.66	87.36	88.88	88.20	90.10	86.70
	DS	93.10	80.46	91.89	95.45	94.00	75.30
	SL	94.25	83.91	97.00	84.84	92.40	83.30
RD	SVM	91.95	83.91	96.80	89.60	89.00	81.00
	DS	93.10	81.61	91.80	88.80	94.00	78.30
	SL	93.10	79.31	94.20	77.10	92.30	80.70
DA	SVM	93.40	81.61	95.10	86.20	93.20	79.30
	DS	93.10	79.31	91.80	85.10	94.00	76.60
	SL	94.25	80.46	97.00	79.40	92.40	81.10

SVM, support vector machine; DS, decision stumps; SL, simple logistic.
All the values are mentioned in percentage.

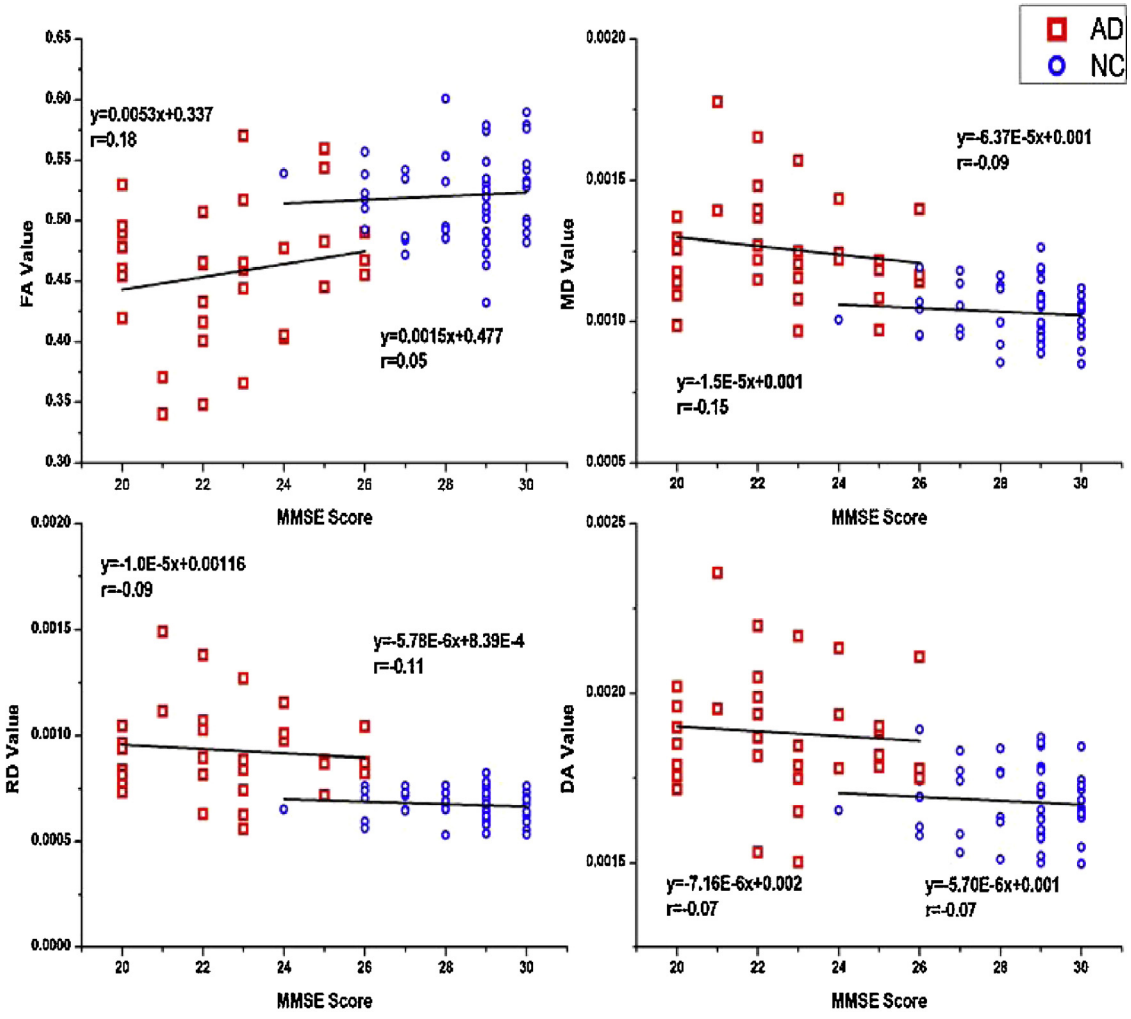

Fig. 3 – Variation of DTI indices with MMSE scores for Splenium of corpus callosum.

Table 5 – Performance evalaution of different approaches in diffrentiating AD from controls.

Method	Features	Number of subjects	Sensitivity	Specificity	Accuracy
Hippo volume	Hippocampus volume	150	63%	80%	71.5%
Hippo-shape	Hippocampal Shape	150	69%	84%	76.5%
Thickness-ROI 90%	Entorhinal cortex, supramarginal gyrus thickness, hippocampal volume	97	69%	94%	81.5%
Gray matter [24]	Gray matter features	31	78.7%	74.3%	76.5%
Multimodal multivariate [24]	Structural and diffusion features	31	99.25%	99.95%	99.60%
Proposed approach	Diffusion and clinical features	87	93.00%	94.40%	94.25%

the regions of distribution for AD and NC are well separated and MMSE score aids in improving the classification performance. This supports the employment of MMSE as a screening tool for dementic disorders.

4. Conclusion

DTI is used to study WM related abnormalities and it is in recent focus to address AD pathology. Use of DTI for diagnosis of AD using sub-anatomic region analysis of WM is in nascent stage and very few reports have been published on this study. It is also noticed that there are conflicting results about correlation between the diffusion indices of sub anatomic regions of WM and MMSE score. For instance Bozzali and Falini [20] reported strong correlation between FA and MMSE score for entire WM regions whereas Ibrahim et al. [21] showed no correlation exist for the same for corpus callosum in AD patients. Also previous studies have suggested MMSE score as a noisy and unreliable [22] tool for cognitive measure of the subjects as it is affected by depression, sleep deprivation, medical conditions and medications. However, in this study MMSE score is found to be the critical indicator of AD pathology and also a significant feature for the classification of AD from NC. To the best of author's knowledge, no study

has been performed considering DTI indices along with MMSE score for classification of AD from NC.

The data is acquired from ADNI repository and preprocessed. Further, diffusion indices are extracted from 50 regions of WM. The observations in this study could be comprehended based on correlation of WM sub-anatomic region analysis of DTI indices with MMSE score and classification of AD vs NC.

Following are the inferences that can be derived from this study:

- There are significant variations in white matter tracts diffusion indices for AD and normal subjects. Micro structural changes are found in Fornix, Splenium of corpus callosum, genu of corpus callosum regions and these variations are quantified by the change in the DTI indices.
- In this sub-anatomic region analysis of DTI indices of WM considering FA, MD, RD and DA no correlation was observed for the indices obtained from significant affected regions of AD with MMSE score.
- Even with conditional statement classifiers such as Decision Stumps classification accuracy close to 90% is attained when the MMSE score is considered along with image features.
- Maximum classification accuracy of 94.25% is achieved when FA along with MMSE score are used as the feature set for SVM classifier.
- Although no correlation exists between diffusion indices of significantly affected regions of WM with MMSE score, still it aids in improving the classification accuracy for AD vs NC.

It shows that image features together with clinical feature have the diagnostic capability to determine AD pathology in isolation. It could be concluded that clinical feature such as MMSE along with image features can be used to build automated tool for classification of AD from NC.

REFERENCES

[1] R. Brookmeyer, E. Johnson, K. Ziegler-Graham, H.M. Arrighi, Forecasting the global burden of Alzheimer's disease, Alzheimer's Dement. 3 (3) (2007) 186–191.

[2] H. Braak, E. Braak, Evolution of neuronal changes in the course of Alzheimer's disease, J. Neural Transm. Suppl. (1998) 127–140.

[3] A.L. Alexander, J.E. Lee, M. Lazar, A.S. Field, Diffusion tensor imaging of the brain, Neurotherapeutics 4 (3) (2007) 316–329.

[4] S. Mori, J. Zhang, Principles of diffusion tensor imaging and its applications to basic neuroscience research, Neuron (2006) 527–539.

[5] M.F. Folstein, S.E. Folstein, P.R. McHugh, Mini-mental state. A practical method for grading the cognitive state of patients for the clinician, J. Psychiatr. Res. (1975) 189–198.

[6] K. Oishi, A. Faria, Atlas-based whole brain white matter analysis using large deformation diffeomorphic metric mapping: application to normal elderly and Alzheimer's disease participants, Neuroimage 46 (2) (2009) 486–499.

[7] L. O'Dwyer, F. Lamberton, A.L.W. Bokde, M. Ewers, Y.O. Faluyi, Using support vector machines with multiple indices of diffusion for automated classification of mild cognitive impairment, PLoS ONE 7 (2) (2012).

[8] M. Granaa, M. Termenona, A. Savioa, Computer aided diagnosis system for Alzheimer disease using brain diffusion tensor imaging features selected by Pearson's correlation, Neurosci. Lett. 502 (2011) 225–229.

[9] J.P. Lerch, A.C. Evans, Cortical thickness analysis examined through power analysis and a population simulation, Neuroimage 24 (2005) 163–173.

[10] L. O'Dwyer, F. Lamberton, A.L.W. Bokde, M. Ewers, Y.O. Faluyi, Using diffusion tensor imaging and mixed-effects models to investigate primary and secondary white matter degeneration in Alzheimer's disease and mild cognitive impairment, J. Alzheimers Dis. 26 (2011) 667–682.

[11] M. Bozzali, A. Falini, et al., White matter damage in Alzheimer's disease assessed in vivo using diffusion tensor magnetic resonance imaging, J. Neurol. Neurosurg. Psychiatry 72 (6) (2002) 742–746.

[12] C.F. Westin, S.E. Maier, H. Mamata, et al., Processing and visualization for diffusion tensor MRI, Med. Image Anal. 6 (2) (2002) 93–108.

[13] M. Jenkinson, C.F. Beckmann, T.E. Behrens, et al., FSL, Neuroimage 62 (2012) 782–790.

[14] B. Thomas, M. Eyssen, R. Peeters, G. Molenaers, P. Van Hecke, Quantitative diffusion tensor imaging in cerebral palsy due to periventricular white matter injury, Brain 128 (2005) 2562–2577.

[15] B.T. Gold, D.K. Powell, A.H. Andersen, C.D. Smith, Alterations in multiple measures of white matter integrity in normal women at high risk for Alzheimer's disease, Neuroimage 52 (2010) 1487–1494.

[16] X. Wu, V. Kumar, J.R. Quinlan, J. Ghosh, Q. Yang, H. Motoda, G.J. McLachlan, A.F.M. Ng, B. Liu, P.S. Yu, Z.-H. Zhou, M. Steinbach, D.J. Hand, D. Steinberg, Top 10 algorithms in data mining, J. Knowl. Inf. Syst. 14 (1) (2008) 1–37.

[17] A.Y. Ng, M.I. Jordan, On discriminative vs. generative classifiers: a comparison of logistic regression and naive Bayes, J. Neural Inf. Process. Syst. (2002), http://ai.stanford.edu/ ang/papers/nips01-discriminativegenerative.pdf.

[18] J. Rennie, Boosting with Decision Stumps and Binary Features, Massachusetts Institute of Technology, Cambridge, MA, 2003 (Technical Report).

[19] R.B. Patil, R. Piyush, S. Ramakrishnan, Identification of brain white matter regions for diagnosis of Alzheimer using diffusion tensor imaging, in: 35th Annual International Conference of the IEEE EMBS, 2013, pp. 6535–6538.

[20] M. Bozzali, A. Falini, White matter damage in Alzheimer's disease assessed in vivo using diffusion tensor magnetic resonance imaging, J. Neurol. Neurosurg. Psychiatry 72 (6) (2002) 742–746.

[21] I. Ibrahim, J. Horacek, A. Bartos, M. Hajek, D. Ripova, M. Brunovsky, J. Tintera, Combination of voxel based morphometry and diffusion tensor imaging in patients with Alzheimer's disease, Neuro. Endocrinol. Lett. 30 (1) (2009) 39–45.

[22] Y.-Y. Chou, N. Leporé, P. Saharan, S.K. Madsen, X. Hua, Ventricular maps in 804 ADNI subjects: correlations with CSF biomarkers and clinical decline, Neurobiol. Aging 31 (2010) 1386–1400.

[23] S. Mori, K. Oishi, H. Jiang, L. Jiang, X. Li, K. Akhter, K. Hua, A.V. Faria, A. Mahmood, R. Woods, A.W. Toga, G.B. Pike, P.R. Neto, A. Evans, J. Zhang, H. Huang, I. Miller, P. van Zijl, J. Mazziotta, Stereotaxic white matter atlas based on diffusion tensor imaging in an ICBM template, Neuroimage 40 (2008) 570–582.

[24] L. Mesrob, M. Sarazin, V. Hahn-Barma, DTI and structural MRI classification in Alzheimer's disease, J. Adv. Mol. Imaging. 2 (2) (2012).